IEEE Access
Multidisciplinary | Rapid Review | Open Access Journal

Received November 16, 2018, accepted December 4, 2018, date of publication December 18, 2018,
date of current version January 29, 2019.

Digital Object Identifier 10.1109/ACCESS.2018.2888488

Enhanced MR Image Classification Using Hybrid Statistical and Wavelets Features

GHAZANFAR LATIF[1,2], (Member, IEEE), D. N. F. AWANG ISKANDAR[2], JAAFAR M. ALGHAZO[1], (Member, IEEE), AND NAZEERUDDIN MOHAMMAD[1], (Member, IEEE)

[1]College of Computer Engineering and Science, Prince Mohammad Bin Fahd University, Khobar 31952, Saudi Arabia
[2]Faculty of Computer Science and Information Technology, University of Malaysia, Kota Samarahan 94300, Malaysia

Corresponding author: Ghazanfar Latif (glatif@pmu.edu.sa)

ABSTRACT Classification of brain tumor is one of the most vital tasks within medical image processing. Classification of images greatly depends on the features extracted from the image, and thus, feature extraction plays a great role in the correct classification of images. In this paper, an enhanced method is presented for glioma MR images classification using hybrid statistical and wavelet features. In the proposed method, 52 features are extracted using the first-order and second-order statistical features (based on the four MRI modalities: Flair, T1, T1c, and T2) in addition to the discrete wavelet transform producing a total of 152 features. The extracted features are applied to the multilayer perceptron (MLP) classifier. The results using the MLP were compared with various known classifiers. The method was tested on the dataset MICCAI BraTS 2015 which is a standard dataset used for research purposes. The proposed hybrid statistical and wavelet features produced 96.72% accuracy for high-grade glioma and 96.04% accuracy for low-grade glioma, which are relatively better compared to the existing studies.

INDEX TERMS MRI classification, glioma tumor, hybrid statistical features, multilayer perceptron.

I. INTRODUCTION

The human brain contains billions of neurons for information processing and body organ operations making it an extremely complex part of the human body. The brain is composed of three part namely; the cerebellum, the brainstem and finally the cerebrum. Surrounded a protective shield known as the skull that is able to protect the brain from injuries and direct damage. The skull cannot, however, protect the brain from internal neurological affects. These affects can cause the most common problem known as tumors. Tumors damage the brain at the cellular level, and thus causing death in most cases. Early detection of tumors and correct diagnosis can assist in early intervention and lifesaving medications and procedures [1].

The Brain MRI uses radio waves, magnetic field and other computing devices to produce images of the brain tissues. Based on magnetic field strength and signal frequency, the Brain MRI can produce four different types of images. The types are; longitudinal relation time (T1) weighted, T1-contrasted, transverse relaxation time (T2) weighted, and fluid-attenuated inversion recovery (Flair) [2]. The different types can be easily identified as tissues in T1 type are dark, tissues in T2 type are bright, and tissues in Flair type clearly shows water and macromolecules. Since MRI depends on the use of magnetic field, it can be used to detect tissue inflammation, bleeding, swelling and tumors.

The early diagnosis and correct classification of brain tumors is extremely important in deciding the type of treatment the patient must undergo. Numerous recent research studies have developed on the design of Convolutional Neural Networks (CNNs) to assist in the process of correct classification of brain tumors based on MR Images. Classifying tumors by physicians is an extremely slow process and is prone to errors. This is one of the main reasons that there has been an increased interest in developing automated highly accurate image processing systems for tumor classification in general, and brain tumor classification in particular [3].

Once a brain abnormality or tumor is detected, it needs to be segmented. However, this is a complex task because MR images are low contrast and highly correlated. This complexity is increased due to the inconsistency of the brain anatomy. Yet correct segmentation is crucial in the proper diagnosis and analysis of the various types of brain tumors.

In this paper, a new technique is proposed in order classify MR Images into tumorous and non-tumorous using feature extraction (enhanced hybrid DWT and statistical features). From each modality, 38 hybrid features have been extracted giving a total of 152 features. The 38 features are based on the first order and second order statistical features in addition to DWT features. The features are applied to various classifiers in order to check the performance of the extracted features. The results achieved show a higher classification accuracy than those mentioned in the existing literature.

The rest of the paper is organized as follows: Section II highlights the previous related literature, Section III details the proposed system, Section IV shows the experimental data (datasets) used, Section V has a detailed discussion on the results, and the paper is concluded in Section VI.

II. LITERATURE REVIEW

The classification technique accuracy is heavily dependent on the feature extraction phase. Various number of features extraction techniques have been proposed such as Gabor features [4], wavelet transform-based features [5], [6], Principle Component Analysis (PCA) [7], and texture features [8] in latest researches. Wavelet transform is a mathematical tool that decomposes the image data into various frequencies used for classification and analysis. Other feature vectors used for classification includes the Duabechies-4 wavelet approximation coefficients [5]. Zhang *et al.* [9] used Fractional Fourier transform based features and support vector machine (SVM) for classification of brain MR images. Using PCA, the features were reduced to 26 features. The experiments were performed on 90 T2-weighted images of size 256×256 and achieved 99.11% accuracy.

Mohsen *et al.* [10] applied Deep Learning combined with Discrete Wavelet Transform (DWT) for the classification of a dataset of 66 brain MRI. Overall, the proposed methodology achieved good results as compared to other methods. Bahadure *et al.* [11] proposed a method which is a combination of Berkeley Wavelet Transform (BWT) along with Support Vector Machine (SVM) for the proper detection, segmentation, and classification of MRI based brain tumor. Their proposed method achieved 96.51% accuracy, a specificity of 94.2%, and sensitivity of 97.72%. Amin *et al.* [12] proposed an automated method to classify cancerous and non-cancerous regions (tumor detection and classification) in MR images. In their proposed method, they apply different method for segmentation. Feature extraction is done based on intensity, texture and shape. SVM classifier is then applied on the MR images for classification. Their proposed method achieve an accuracy of 97.1%, specificity of 98% and sensitivity of 91.9%. The method was tested on three different datasets namely; Local, RIDER, and Harvard. Shenbagarajan *et al.* [13] propose an efficient MRI brain analysis technique. The technique utilizes the use of Active Contour Method (ACM) for segmentation and classification is done using Artificial Neural Network (ANN) based on Levenberg-Marquardt (LM) algorithm. Their proposed method was reported to produce excellent results with an accuracy of 93.74%. Zhou *et al.* [14] proposed a detection of pathological brain from Brain MR Images based on Wavelet-Entropy and Naïve Bayes Classifier. Their method achieved an accuracy of 92.6%, a specificity of 91.7% and a sensitivity of 94.5% when applied to a dataset of 64 images. Gurusamy and Subramaniam [15] proposed a simple and efficient method for brain MR image classification that consisted of Feature extraction bas on color moments and classification using Artificial Neural Network (ANN). With this simple method, they achieved fairly good results with an overall accuracy of 91.8% when applied to a dataset consisting of 70 images (25 normal and 45 abnormal).

Aerts *et al.* [16] propose a radiomic analysis procedure consisting of 440 features to quantify the tumorous image shape, intensity, and texture extracted from a dataset of 1,019 patients image of lung or head/neck cancer. Datasets used in the study were lung1, lung2, H&N1 and H&N2. Their method proved that noninvasive techniques can be used to diagnose whether a patient has a tumor or not based on this radiomic analysis procedure. Li *et al.* [17] propose radiomic analysis to identify the MR image features linked with epidermal growth factor (EGFR) expression level in lower grade gliomas. They used a data set consisting of 270 lower grade Glioma patients with known EGFR expression status. 25 wavelet features were proposed in their method which achieved an accuracy of 82.5%.

Corso *et al.* [18] used multimodal brain dataset of 20 expert's annotated glioblastoma multiform (GBM) gathered from different sources. Pre-processing is performed on all the four modalities T1, T1C, T2 and FLAIR. A top-down model based approach is used to distribute the product over a generative model, where classification and segmentation are performed. In the second step, a sparse graph is input to the graph cut method. The graph cut method uses segmentation by weighted aggregation (SWA) to provide the multi-level segmentation of data, where each voxel is classified into one of the three (active tumor, necrotic or edema) classes and at a higher level these voxels are combined as a single segment. Automatic classification is performed using the random forest (RF) [19], where features extraction is performed after pre-processing. Features for classification include MR sequence intensities, neighborhood information, context information and texture.

A three-stage process is presented in [20] to find abnormalities in brain MRI scans. The authors have used various techniques such as feature extraction, image transformation and image segmentation by using fuzzy logic to evaluate the overall quality of proposed method. Two metrics i.e. False Alarm (FA) and Missed Alarm (MA) are used to calculate the performance of detected brain tumor images. The results are compared with various existing methods used for the tumor detection and the proposed method gives relatively smaller values of FA. The MA values, however, are high because the method is not able to handle the symmetry of brain tumor around the center vertical line.

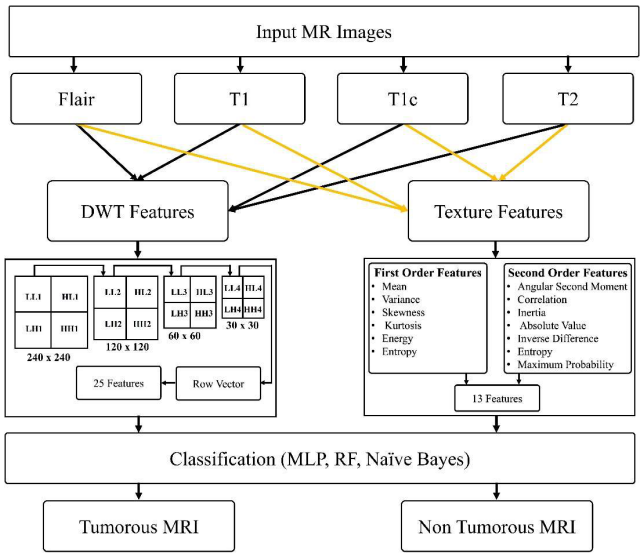

FIGURE 1. Proposed system for MR Image classification.

Jaffar *et al.* [21] proposed a different technique that uses fuzzy curvelets, Discrete Cosine Transform (DCT) and Support Vector Machines to categorize the MR images as benign (non-cancerous) and malignant (cancerous). In initial stages, noise is removed from the images using fuzzy curvelets and features are extracted from the denoised image using DCT. Afterwards, the features are fed to an SVM for classification. Fuzzy based clustering algorithms are used to segment the images and detect brain tumor. A comparison of different image transformation techniques, to extract tumor features from MR image, is provided in [22]. The authors de-noise image in the initial stage and use DCT and DWT to obtain relevant characteristics of the input image, which are later segmented using neural network techniques to find the brain irregularities. Sensitivity and accuracy metrics are used to study the performance of DCT and DWT on tumor detection.

A multi-layer architecture for tumor classification is presented in [23]. Once the initial filtering (noise removal) is complete, various feature sets of the input image are obtained using the histogram and matrix-based systems. Normal and abnormal images are separated using a random forest classifier. The abnormal images are further separated into glioma and meningioma which helps in tumor segmentation using active contour model and bounding box. The method achieved an accuracy of 87.62 %.

III. PROPOSED SYSTEM

The proposed technique consists of various stages which is shown in Fig. 1. The MR Image is given as input to the system and subsequently the stage of feature extraction (FE) is applied to the MR image. The feature extraction stage utilizes the statistical and DWT feature extraction techniques. The MR image then goes through the classification phase which classifies the image as either tumorous or non-tumorous based on the extracted features. If the image is classified as benign, then no additional processing is required. However, if the image is classified as malignant, then the image will be passed to the next stage of segmentation to extract the tumorous portion. The details of the different stages in the proposed system are discussed below.

A. FEATURE EXTRACTION

Feature extraction describes the process of converting the input images into unique set of useful feature sets. In other words, it is a way of reducing the dimensionality of raw images into a concise set of desirable features. A good set of extracted features make the task of formal classification technique easy in classifying the images. However, the extraction of useful distinctive features is a complex and tedious task. There are several well-known techniques for feature extraction including local binary patterns, transform features, principal component analysis, decision boundary feature extraction and statistical features.

Characterization of brain tumor images require careful extraction of useful image features which are given as an input for the image classification methods. For this purpose, a hybrid technique using statistical and DWT features is proposed in this paper. The details of these feature extraction techniques is described below.

1) STATISTICAL FEATURES

Statistical can be thought as a recurrent pattern of information or structure in raw data. There are different ways to extract the statistical features such as, structural, statistical, and transform based methods. In this paper statistical based feature extraction methods are used, specifically it focused on first order histogram based features and second order co-occurrence matrix features from MR images.

Histogram provides First order statistical information for the images. Probability density (P) can be used as a measure of the occurrence of the intensity level. This can be calculated by using (1) [24].

$$P(i) = \frac{I(m)}{N}, \quad m = 1, \ldots, L \tag{1}$$

where I refers to intensity level histogram values, N refers to the total number pixels which is product of the horizontal spatial domain resolution cells (H) and the vertical spatial domain resolution cells (V). $I(m)$ is the intensity level for a given gray scale level m; L is the maximum number of gray levels in an input image.

From probability density of gray scale intensity levels (P) several useful quantitative first order statistical features can be obtained. These features include mean (F_1), variance (F_2), skewness (F_3), kurtosis (F_4), energy (F_5) and entropy (F_6). The first simple feature *mean* represents the average of the MRI intensity, while *variance* measures the intensity changes around the mean. The degree of asymmetry around the mean of the histogram is measured by the *skewness*. The degree of outliers in the histogram are measured by the *kurtosis*, uniformity of histogram is measured by the *energy*, and the randomness of distribution is measured by *entropy*.

The mathematical formulas of these first order statistical features using probability distribution of intensity levels are shown in (2-7).

$$F_1 = \sum_{m=1}^{L} mP(m) \tag{2}$$

$$F_2 = \sum_{m=1}^{L} (m - F_1)^2 P(m) \tag{3}$$

$$F_3 = \sigma^{-3} . \sum_{m=1}^{L} (m - F_1)^3 . P(m) \tag{4}$$

$$F_4 = \sigma^{-4} . \sum_{m=1}^{L} (m - F_1)^4 . P(m) - 3 \tag{5}$$

$$F_5 = \sum_{m=1}^{L} P(m)^2 \tag{6}$$

$$F_6 = -\sum_{m=1}^{L} P(m) \log_2 P(m) \tag{7}$$

where, $P(i)$ is the probability density obtained in (1) and $m = 1, 2, \ldots, L$. σ is standard deviation which is $\sqrt{F_2}$.

The first order statistical features based on Histogram are considered local features. They do not take into account the spatial information that can be obtained from the image. Therefore, a second level of feature extraction utilizes the gray-level spatial co-occurrence matrix $[M(m, n)]$. These features have been defined as the second order histogram based features, and are calculated using the joint probability distribution of pixel pairs [25]. The joint probability distribution between pixels uses the distance (d) and angle (O) within a given neighborhood as a basis for the calculation [26]. It is the practice to use d $= 1, 2$ and $\theta = 0°, 45°, 90°, 135°$ for calculation of the joint probability distribution between pixels. Statistical features derived from the matrix are Angular Second Moment Energy (F_7), Correlation (F_8), Inertia (F_9), Absolute Value (F_{10}), Inverse Difference (F_{11}), Entropy (F_{12}) and Maximum Probability (F_{13}) can be calculated as shown in (8-14).

$$F_7 = \sum_{m=0}^{L} \sum_{n=0}^{L} [P(m, n)]^2 \tag{8}$$

$$F_8 = \sum_{m=}^{L} \sum_{n=0}^{L} \frac{m.n.P(m, n) - \mu_x \mu_y}{\sigma_x \sigma_y} \tag{9}$$

$$F_9 = \sum_{m=1}^{L} \sum_{n=1}^{L} (m - n)^2 . P(m, n) \tag{10}$$

$$F_{10} = \sum_{m=1}^{L} \sum_{n=1}^{L} |m - n| . P(m, n) \tag{11}$$

$$F_{11} = \sum_{m=1}^{L} \sum_{n=1}^{L} \frac{P(m, n)}{1 + (m - n)^2} \tag{12}$$

$$F_{12} = -\sum_{m=1}^{L} \sum_{n=1}^{L} P(m, n) . \log_2 P(m) \tag{13}$$

$$F_{13} = P(m, n)) \tag{14}$$

A total of thirteen first and second order statistical features are extracted.

2) DISCRETE WAVELET FEATURES

Wavelet transform refers to time-frequency decomposition of signals into basic functions called wavelets. Wavelets are purposefully derived to hold specific properties which are useful in image processing. Wavelet coefficients are employed as feature vectors for image classification. Discrete Wavelet Transform (DWT) is a feature extraction method using a discrete set of the wavelet scales and translations. It is used for efficient and quick de-noising of a noisy signal. Its implementation is regarded as computationally efficient [27].

The DWT transforms a one variable function into a function of two variables, which are translation and scale. The wavelet coefficients are calculated at discrete scales based on powers of two.

$$W_{j,k}(n) = \sum_j \sum_k x(k) 2^{-j/2} \Psi(2^{-j} n - k) \tag{15}$$

The discrete function $x(k)$ can be represented as a detailed component (weighted summation of wavelets) plus a coarse approximation. The coarse approximation is further decomposed by iterative low pass and high pass filtering of the time domain signal. The approximation and detailed components (a_j and d_j) are calculated as shown in (16-17).

$$a_{j+1}[k] = \sum_{m=-\infty}^{+\infty} l[m - 2k] a_j[m] \tag{16}$$

$$d_{j+1}[k] = \sum_{m=-\infty}^{+\infty} h[m - 2k] a_j[m] \tag{17}$$

The sequences $l[m - 2k]$ and $h[m - 2k]$ are low pass and high pass filters obtained from the original wavelet.

DWT is used for numerical and functional analysis in data compression, image processing, and signal processing. In DWT, image is divided into different frequencies using linear transformation. The four sub-bands generated are HH, HL, LL, and LH, where HH, LH, and HL represent detail coefficients and LL is for approximate coefficients. In proposed model the brain MRI features are extracted using level 3 DWT. Fig. 2 show the process of 3 level DWT approximation and detailed coefficients. For this study, a total of 25 features are extracted using DWT.

3) CLASSIFICATION

Classification is the process of classifying the input patterns into analogous classes. The selection of suitable classifier is dependent on the accuracy, performance and time complexity. The proposed hybrid features are tested using three different classifiers named; Multilayer Perceptron, Naïve Bayes and Random Forest [28]. The proposed hybrid features set got better results through all the classifiers but MLP got the highest accuracy. Several experiments are performed on the acquired MICCAI BraTS 2015 datasets for binary classification [29].

IV. EXPERIMENTAL DATA

For experiments, a worldwide recognized MRI dataset named MICCAI brain tumor image segmentation (BraTS) 2015 [29]. The dataset contains training and testing samples of both Low-grade Glioma (LGG) and High-grade Glioma (HGG). In the experiments, total 39 cases of HGG and 26 cases of LGG are selected randomly and used as described in the Table 1. Each training sample has 155 MRI slices for each T1, T2, T1c, Flair and annotated (Labeled) images. Similarly, there are 110 samples in the testing dataset. Each

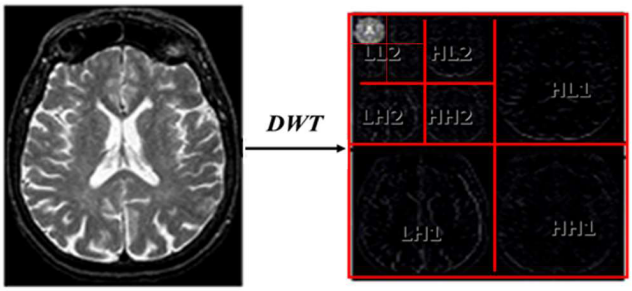

FIGURE 2. DWT 3 level for Brain MRI.

TABLE 1. Description of BraTS dataset used in experiments.

	HGG	LGG	Total
Number of Experiment Cases	39 Cases	26 Cases	65 Cases
Number of Sequence Modalities	4 Types	4 Types	4 Types
Total Number of MR Images	24,180	16,120	40,300
Tumorous MR Images in each Sequence Type	1,551	2,879	4,430
Non-tumorous MR Images in each Sequence Type	2,169	2,081	4,250
Pixel Size of each MR Image	240×240	240×240	240×240

testing dataset also has T1, T2, T1c and Flair images, each one having 155 images. In order to validate the results, two other datasets were used in the study. A dataset published by Harvard Medical School named AANLIB was used and consists of 90 MR images divided into 62 normal cases and 28 tumorous images [28]. Another dataset used for validation is the Pakistan Institute of Medical Sciences (PIMS) dataset that consists of 144 normal images and 114 tumorous images with a total size of 258 images [30]. In the BraTS dataset, only 65 cases were used for the purpose of this study. The 65 cases contained 40,300 images for all four modalities which is sufficient to provide the statistical required for the proper operation and verification of the proposed technique. The total BraTS dataset was not used because of the limited computer resources, however, this should not affect the overall analysis and performance of the proposed method.

V. RESULTS AND DISCUSSIONS

The usefulness of extracted statistical and DWT features is studied using four well known classifiers, namely Random Forest (RF), Multilayer Perceptron (MLP), Naïve Bayes (NB) and Support Vector Machines (SVM). RF is supervised classification method that uses decision trees, but it randomly finds the root node and splits the feature nodes. RF with enough trees has an advantage of avoiding the overfitting problem. It also has ability to handle missing values in the data. MLP is an artificial neural network (ANN) based classification method. Other ANN techniques were also tested, but didn't offer any comparable accuracy. The Naive Bayes model is chosen for this study because of its simplicity, ability to analyze huge data sets, and proven history of outperforming highly sophisticated classification methods. SVM is a supervised machine learning algorithm, which uses the kernel trick to transform the classification data and then implicitly finds an optimal boundary between the possible outputs. It is well-known for superior accuracy for non-linear classifications. All of the above classifiers are tested for:

A. Each MRI modality using statistical and DWT feature sets separately.
B. Each MRI modality using combined statistical and DWT feature sets.
C. Combined MRI Modalities and combined feature sets.

All these experiments are done on LGG and HGG samples separately. For each experiment, accuracy of the classification is measured. Additionally, other performance measures (precision, recall, F1 measure, and ROC) are also calculated to show fidelity of results. Accuracy refers to the fraction of classifications that are predicted correctly; precision is the fraction of positive identifications that are actually correct; recall refers to the fraction of actual positives classified; F1 is the harmonic mean of precision and recall score, which is product of these two scores over sum of them; ROC (receiver operating characteristic) is performance classification method at different thresholds.

The classification results of MLP, RF, SVM and NB for the three different cases are discussed in the following subsections. For comprehensibility the results are discussed based on the accuracy of the classifiers. However, the other performance measures (precision, recall, ROC and F1) followed similar trends as accuracy. It should be noted that the experiments are conducted with different set of classifier parameters. The parameters with better accuracy were chosen and their results are presented in this paper. In MLP, the number of hidden layers is set to (Number of Features + Classes) / 2, momentum weights value is chosen as 0.2, and training epochs are chosen as 500. The learning weights are updated with a learning rate of 0.3. For RF classifier, the number of randomly chosen attributes is set to integer value of (log_2(number of predictors) + 1), and 100 iterations are performed. For SVM, a type C-SVC SVM with linear kernel type is used. The batch size of 100 is chosen for all classifiers.

A. SEPARATE FEATURE SETS FOR INDIVIDUAL MRI MODALITIES

Table 2 shows the results obtained for LGG and HGG samples for different feature types of different MRI Modalities and classifiers. The first half columns of the table shows the results obtained from HGG samples. The results show that RF classifier produced the best results using the feature sets extracted from flair modality. Statistical features produced 92.3% accuracy, whereas the DWT features produced 88.4% accuracy. In other words, statistical features of

TABLE 2. Experimental results for LGG and HGG against different feature types of different MRI modalities and classifiers.

			DWT Features					Statistical Features				
			Accuracy	Precision	Recall	F Measure	ROC	Accuracy	Precision	Recall	F Measure	ROC
HGG	RF	Flair	**88.39**	**0.883**	**0.919**	**0.900**	**0.944**	**92.30**	**0.921**	**0.947**	**0.934**	**0.973**
		T1	71.01	0.758	0.724	0.741	0.792	85.41	0.888	0.853	0.870	0.934
		T1c	72.82	0.753	0.781	0.767	0.819	86.87	0.885	0.885	0.885	0.942
		T2	80.74	0.813	0.862	0.836	0.890	88.63	0.886	0.919	0.902	0.950
	MLP	Flair	88.03	0.876	0.922	0.898	0.941	87.38	0.888	0.894	0.890	0.940
		T1	72.17	0.783	0.715	0.745	0.804	82.28	0.880	0.800	0.837	0.896
		T1c	65.49	0.841	0.489	0.618	0.734	83.29	0.853	0.856	0.854	0.906
		T2	79.93	0.795	0.876	0.833	0.880	85.56	0.864	0.888	0.875	0.927
	Naïve Bayes	Flair	62.40	0.807	0.450	0.577	0.698	75.60	0.907	0.639	0.749	0.862
		T1	64.44	0.805	0.499	0.616	0.711	76.52	0.910	0.655	0.761	0.847
		T1c	65.49	0.841	0.489	0.618	0.734	75.74	0.905	0.643	0.752	0.842
		T2	69.70	0.899	0.530	0.666	0.853	76.73	0.912	0.657	0.763	0.857
	SVM	Flair	85.93	0.842	0.928	0.883	0.848	82.71	0.899	0.786	0.839	0.834
		T1	69.89	0.676	0.907	0.775	0.664	57.15	0.572	1.000	0.727	0.500
		T1c	56.54	0.570	0.978	0.720	0.497	59.60	0.590	0.961	0.731	0.536
		T2	59.60	0.590	0.961	0.731	0.536	78.25	0.801	0.825	0.813	0.775
LGG	RF	Flair	81.87	0.837	0.856	0.846	0.896	**89.94**	**0.902**	**0.928**	**0.915**	**0.957**
		T1	72.51	0.770	0.754	0.762	0.806	87.33	0.886	0.898	0.892	0.940
		T1c	72.86	0.777	0.750	0.763	0.804	88.62	0.903	0.902	0.902	0.951
		T2	79.25	0.791	0.875	0.831	0.880	89.89	0.893	0.940	0.915	0.956
	MLP	Flair	**82.19**	**0.837**	**0.863**	**0.849**	**0.890**	86.46	0.876	0.896	0.885	0.931
		T1	74.21	0.803	0.742	0.770	0.818	83.73	0.849	0.880	0.863	0.905
		T1c	74.84	0.845	0.698	0.763	0.816	83.74	0.842	0.890	0.865	0.921
		T2	78.16	0.770	0.896	0.827	0.868	84.22	0.842	0.901	0.869	0.924
	Naïve Bayes	Flair	60.69	0.857	0.390	0.536	0.702	76.97	0.923	0.660	0.769	0.856
		T1	59.34	0.814	0.392	0.529	0.666	77.27	0.916	0.672	0.775	0.868
		T1c	62.38	0.816	0.458	0.586	0.719	78.47	0.919	0.692	0.789	0.870
		T2	67.82	0.836	0.557	0.668	0.816	77.16	0.915	0.670	0.774	0.874
	SVM	Flair	63.35	0.813	0.482	0.605	0.664	80.62	0.885	0.768	0.822	0.814
		T1	70.51	0.863	0.587	0.699	0.728	78.88	0.798	0.853	0.825	0.776
		T1c	70.14	0.828	0.615	0.706	0.718	74.04	0.731	0.876	0.797	0.714
		T2	73.73	0.792	0.745	0.768	0.736	78.81	0.838	0.789	0.813	0.788

flair modality produced 3.91% more accuracy than the DWT features.

MLP also produced similar result patterns as RF, that is, statistical features using flair modality produced better results that the other feature sets. MLP performance using flair modality's DWT feature sets is similar to RF. It has around 0.31% less accuracy than the RF results. However, the difference is much higher (4.92%) when statistical feature sets are used. SVM accuracy is less than RF and MLP accuracy in all cases. NB classifier produced very low accuracy. The best accuracy (76.73%) is achieved using the statistical feature set of T2 modality, which is 15% less than the accuracy obtained using RF classifier. So, if the choice of feature sets is restricted then it is better to choose the statistical features extracted from the flair modality.

The second half of Table 2 shows the results obtained using LGG sample set. RF classifier results have similar pattern as in the case of HGG. Statistical feature sets of Flair modality produced best accuracy. In case of DWT feature sets, MLP has produced accuracy of 82.19% which is slightly (0.32%) better than RF's accuracy. As in the case of HGG, SVM and NB classifiers produced inferior results for all feature sets. NB has the least accuracy and its accuracy is 11.47% less than the best accuracy obtained.

TABLE 3. Experimental results for LGG and HGG against combined feature types of different MRI modalities and classifiers.

			Combined (Statistical and DWT) Features				
			Accuracy	Precision	Recall	F Measure	ROC
BraTS HGG	RF	Flair	**95.09**	**0.936**	**0.981**	**0.958**	**0.986**
		T1	85.74	0.889	0.858	0.873	0.936
		T1c	87.82	0.887	0.903	0.894	0.946
		T2	89.01	0.887	0.926	0.906	0.957
	MLP	Flair	94.81	0.942	0.969	0.955	0.981
		T1	82.88	0.871	0.824	0.846	0.909
		T1c	86.04	0.861	0.901	0.881	0.935
		T2	88.38	0.880	0.923	0.901	0.946
	Naïve Bayes	Flair	64.20	0.859	0.447	0.588	0.829
		T1	69.75	0.878	0.547	0.674	0.812
		T1c	70.02	0.916	0.524	0.666	0.838
		T2	73.39	0.922	0.585	0.715	0.876
	SVM	Flair	83.62	0.862	0.850	0.856	0.834
		T1	80.40	0.815	0.850	0.832	0.796
		T1c	78.99	0.838	0.784	0.810	0.791
		T2	78.99	0.805	0.835	0.820	0.782
BraTS LGG	RF	Flair	92.88	0.927	0.953	0.940	0.978
		T1	87.64	0.895	0.892	0.894	0.948
		T1c	89.14	0.910	0.903	0.906	0.952
		T2	92.20	0.918	0.951	0.934	0.971
	MLP	Flair	**93.46**	**0.930**	**0.961**	**0.945**	**0.975**
		T1	85.33	0.854	0.904	0.878	0.924
		T1c	87.23	0.887	0.896	0.891	0.938
		T2	91.38	0.913	0.943	0.927	0.960
	Naïve Bayes	Flair	64.66	0.916	0.433	0.588	0.828
		T1	63.89	0.864	0.451	0.593	0.819
		T1c	70.60	0.912	0.548	0.685	0.853
		T2	73.25	0.895	0.613	0.727	0.868
	SVM	Flair	77.52	0.776	0.864	0.817	0.758
		T1	78.56	0.790	0.862	0.824	0.771
		T1c	80.17	0.895	0.747	0.814	0.813
		T2	79.18	0.806	0.847	0.826	0.781

Overall HGG sample sets produced better accuracy than LGG sample sets, and statistical feature sets produced better results than DWT feature sets. In the next set of experiments, we mixed DWT and statistical feature sets.

B. HYBRID FEATURE SETS FOR INDIVIDUAL MRI MODALITIES

In this subsection, the classification results obtained after combining DWT and statistical feature sets is studied. The resultant hybrid set after merging two feature sets has a total of 38 features for each MRI modality. The obtained results from RF, MLP, SVM and NB classifiers are summarized in Table 3.

RF classifier produced best accuracy for HGG samples using hybrid feature sets of flair modality. It has an improved accuracy of 95.09%, which is 2.79% higher than the accuracy obtained with segregated DWT and statistical feature sets. MLP classifier has also achieved an improved accuracy of 94.89% with hybrid feature sets, which is 6.78% higher than the accuracy obtained with separate feature sets. MLP accuracy is only 0.28% less than the accuracy obtained by RF classifier.

Similar to HGG dataset, the classification accuracy on LGG dataset using MLP and RF classifiers has improved. However, in this case MLP has produced better results than RF; its accuracy is 0.58% better than RF accuracy. NB classifier is an exception; its accuracy has decreased using hybrid feature sets. Its accuracy is 3.39% and 5.16% less than the best accuracy obtained by separate feature sets for HGG and LGG dataset respectively.

TABLE 4. Experimental results for LGG and HGG against combined MRI modalities feature sets and different classifiers.

			Combined (Flair, T1, T1c, T2) Features				
			Accuracy	Precision	Recall	F Measure	ROC
HGG	RF	DWT	93.37	0.917	0.972	0.944	0.978
		Statistical	95.77	0.951	0.977	0.964	0.990
		DWT + Statistical	96.21	0.953	0.983	0.967	0.992
	MLP	DWT	93.70	0.936	0.956	0.945	0.975
		Statistical	93.94	0.947	0.947	0.947	0.977
		DWT + Statistical	**96.72**	**0.965**	**0.978**	**0.971**	**0.991**
	Naïve Bayes	DWT	66.60	0.898	0.469	0.616	0.821
		Statistical	76.03	0.909	0.646	0.755	0.850
		DWT + Statistical	70.42	0.922	0.527	0.671	0.872
	SVM	DWT	81.72	0.796	0.915	0.851	0.801
		Statistical	84.70	0.900	0.823	0.860	0.851
		DWT + Statistical	85.51	0.830	0.939	0.881	0.841
LGG	RF	DWT	91.04	0.897	0.956	0.926	0.968
		Statistical	94.74	0.942	0.969	0.956	0.981
		DWT + Statistical	95.71	0.949	0.979	0.964	0.988
	MLP	DWT	90.87	0.906	0.942	0.923	0.963
		Statistical	93.97	0.940	0.959	0.949	0.973
		DWT + Statistical	**96.04**	**0.960**	**0.973**	**0.966**	**0.990**
	Naïve Bayes	DWT	61.87	0.894	0.392	0.545	0.792
		Statistical	77.42	0.922	0.669	0.775	0.871
		DWT + Statistical	69.20	0.948	0.499	0.653	0.873
	SVM	DWT	77.52	0.776	0.864	0.817	0.758
		Statistical	82.61	0.813	0.910	0.859	0.809
		DWT + Statistical	82.98	0.856	0.851	0.854	0.826
Combined (LGG+HGG)	RF	DWT + Statistical	96.68	0.958	0.985	0.972	0.992
	MLP	DWT + Statistical	**96.73**	**0.969**	**0.974**	**0.972**	**0.993**
	Naïve Bayes	DWT + Statistical	85.26	0.836	0.926	0.879	0.840
	SVM	DWT + Statistical	72.21	0.945	0.549	0.695	0.894

MLP has the best combined overall accuracy, which moderately more than RF accuracy. Also, it can be easily reasserted that hybrid feature sets contribute the most towards the classification accuracy in MLP and RF classifiers. NB is an exception where statistical feature sets have more influence than the hybrid feature sets.

C. HYBRID FEATURES AND MIXED MRI MODALITIES

In this subsection we study the performance of classification algorithms after combining all four MRI modalities for DWT, statistical, and hybrid feature sets. Table 4 shows the results for both HGG and LGG datasets. Mixing MRI modalities has improved the accuracy of RF and MLP classifiers regardless of feature sets (statistical, DWT, and hybrid) and datasets (HGG and LGG). However, hybrid feature set produced the best results. The accuracy improvements for RF, MLP, and SVM using hybrid feature set are 1.12%, 1.91% and 1.81% respectively for HGG dataset, while the performance enhancement for LGG dataset are 2.83%, 2.58% and 2.81% respectively. This clearly implies that merging data of different modalities is beneficial for classification. Again the only exception is NB classifier, which hasn't shown any improvement.

D. PROCESSING TIME OF CLASSIFIERS

The analysis of results in the previous subsections clearly shows that MLP has better accuracy than the other compared classifiers when hybrid feature sets of merged modalities are used. In this subsection, the accuracy is compared with respect to the total CPU processing time needed for training and testing classifiers. Table 5 summarizes the average processing time of MLP, NB, SVM and RF classifiers for different MRI Modalities against different feature sets and datasets. From these results, it can be concluded that NB classifier is most efficient as it requires the least amount of time. However, its accuracy is very low when compared to the other classifiers.

SVM required a high processing time except for the few cases such as ''DWT features with combined modalities'', where MLP needed the highest processing time. However, SVM accuracy is very low when compared to MLP and RF. So, SVM is not a good choice for this classification problem.

TABLE 5. Average processing time of LGG and HGG for different MRI modalities against different feature sets and classifiers.

	HGG				LGG			
	MLP	SVM	Naïve Bayes	RF	MLP	SVM	Naïve Bayes	RF
DWT Features (Average)	22.3874	153.86	0.0446	3.848	14.9061	88.62	0.0348	2.2074
Statistical Features (Average)	8.1816	259.53	0.0234	2.1514	5.438	26.06	0.0153	1.1993
DWT + Statistical (Average)	47.6686	440.95	0.0742	3.0919	31.8114	32.75	0.0422	1.2591
DWT Combined all Modalities	287.311	179.40	0.1893	7.3237	191.927	108.85	0.125	2.5315
Statistical Combined all Modalities	83.533	214.64	0.0987	3.0096	55.643	45.862	0.0639	1.8219
DWT + Statistical Combined all Modalities	660.722	494.20	0.289	4.9818	436.086	174.313	0.2001	2.7799

TABLE 6. Experimental results for external validation datasets (PIMS and AANLIB).

Dataset	Features	Classifier	Accuracy	Precision	Recall	F Measure	ROC
AANLIB	DWT Features	RF	100	1	1	1	1
		MLP	**100**	**1**	**1**	**1**	**1**
		Naïve Bayes	100	1	1	1	1
		SVM	70.59	0.706	1	0.828	0.500
	Statistical Features	RF	94.12	0.923	1.000	0.960	1.000
		MLP	94.74	1.000	0.923	0.960	0.936
		Naïve Bayes	94.74	1.000	0.923	0.960	0.923
		SVM	68.42	0.684	1.000	0.813	0.500
	Combined (Statistical and DWT) Features	RF	100	1	1	1	1
		MLP	**100**	**1**	**1**	**1**	**1**
		Naïve Bayes	100	1	1	1	1
		SVM	94.74	0.929	1	0.963	0.917
PIMS	DWT Features	RF	82.69	0.917	0.759	0.830	0.908
		MLP	**84.62**	**0.957**	**0.759**	**0.846**	**0.940**
		Naïve Bayes	71.15	0.733	0.759	0.746	0.778
		SVM	69.23	0.697	0.793	0.742	0.679
	Statistical Features	RF	90.38	0.962	0.862	0.909	0.952
		MLP	**92.31**	**0.879**	**1.000**	**0.935**	**0.997**
		Naïve Bayes	65.38	0.867	0.448	0.591	0.756
		SVM	55.77	0.571	0.828	0.676	0.522
	Combined (Statistical and DWT) Features	RF	92.31	0.963	0.897	0.929	0.962
		MLP	**98.08**	**1.000**	**0.966**	**0.982**	**1.000**
		Naïve Bayes	65.38	0.628	0.931	0.750	0.618
		SVM	75.00	0.767	0.793	0.780	0.810

Processing time needed for MLP is also very high when compared to RF classifier in all cases. It took 660.722 and 436.086 seconds for hybrid feature set of combined modalities on HGG and LGG datasets respectively, which is 132 and 156 times more than the time taken by RF classifier. However, the improvement in accuracy offered by MLP is only 0.51% and 0.33% more than RF classifier on HGG and LGG datasets. In other words, RF is a good choice when quick classification is needed and/or devices are resource constrained.

E. RESULTS VALIDATION AND COMPARISON

Machine learning algorithms could over fit the data, and hence an independent validation is necessary. For this purpose, we used two independent datasets AANLIB and PMIS. AANLIB dataset [30], available on Harvard Medical School website, consists of 90 flair modality MR Images with 62 normal and 28 tumorous images. PIMS (Pakistan Institute of Medical Sciences) dataset [28] consists of 258 T1 modality MR images including 144 normal and 114 tumorous images. The obtained results using these two datasets for all four aforementioned machine learning approaches are shown Table 6. The results show that for AANLIB dataset DWT features are more useful than statistical features. RF, MLP and NB classifiers achieved 100% accuracy using DWT features. SVM classifier produced nominal accuracy of 70.59% with DWT features. Its accuracy was improved to 94.74% with combined statistical and DWT features. Conversely, the statistical features turned out be more useful than the DWT features for PIMS dataset. RF and MLP classifiers obtained around 8% higher accuracy using the statistical features than DWT features. Combining DWT and statistical features further improved the accuracy of RF and MLP classifiers. MLP has achieved the highest accuracy of 98.09%.

TABLE 7. Comparison of proposed method with the other methods in the literature.

Method	Data (Images)	Accuracy
Proposed Method (Statistical + DWT, MLP) with AANLIB dataset	90	100%
Proposed Method (Statistical + DWT, MLP) with PIMS dataset	258	98.08%
Proposed Method (Statistical + DWT, MLP) with BraTS dataset	40,300	96.73%
Mohsen et al., 2018, (DWT+PCA+DNN) [10]	66	96.97%
Bahadure et al., 2017, (BWT+SVM) [11]	179	96.51%
Amin et al., 2017, (Texture +SVM) [12]	185	97.1%
Shenbagarajan et al., 2016, (ANNLM) [13]	80	93.74%
Zhou et al., 2015, (Entropy + NBC) [14]	64	92.60%
Nazir et al., 2015 (Color Moments + FFNN) [31]	70	91.8%
Havaei et al., 2014 (kNN-CRF) [32]	40	86.00%

The validation results reaffirm the finding that combined DWT and statistical features produce higher accuracies with both RF and MLP classifiers.

Table 7 shows a quick comparison of our results with the other published results in the literature. The first column of the table shows the research study details along with features and classification techniques used. The other two columns show the number of images used and classification accuracy obtained. It evident that the classification accuracy of proposed method is better than the existing studies. Machine learning techniques rely on statistical information and features obtained from datasets that contain large number of images. Some recent research studies have used datasets that contain a small number of images which makes their results unreliable. The accuracy obtained with our proposed approach even when using a big dataset (40300 images) is very high, which shows the robustness of the approach.

VI. CONCLUSION

A new method for brain glioma tumor classification is proposed in this paper. The classification of MR Images into tumorous and non-tumorous images is performed based on features extracted using first order and second order statistical features and DWT features. A total of 152 features are produced for both HGG and LGG images. The proposed features were then input to the classification phase with MLP chosen as the classifier. However, the features were also studied with various other well-known classifiers for comparison purposes. Results indicate that proposed method achieved 96.72% accuracy for HGG and 96.04% accuracy for LGG. The dataset used in this study is the MICCAI BraTS 2015 which is a well-known and widely used dataset. The results achieved in this work are better than those reported in the literature review. Future work will concentrate on deep learning algorithms for feature extraction in order to achieve a higher accuracy of classification for brain tumor MR Images.

REFERENCES

[1] El-S. A. El-Dahshan, H. M. Mohsen, K. Revett, and A.-B. M. Salem, "Computer-aided diagnosis of human brain tumor through MRI: A survey and a new algorithm," *Expert Syst. Appl.*, vol. 41, no. 11, pp. 5526–5545, Sep. 2014.

[2] R. Meier, S. Bauer, J. Slotboom, R. Wiest, and M. Reyes, "A hybrid model for multimodal brain tumor segmentation," *Multimodal Brain Tumor Segmentation*, vol. 31, pp. 31–37, Aug. 2013.

[3] P. Afshar, A. Mohammadi, and K. N. Plataniotis. (2018). "Brain tumor type classification via capsule networks." [Online]. Available: https://arxiv.org/abs/1802.10200

[4] S. Arivazhagan, L. Ganesan, and S. P. Priyal, "Texture classification using Gabor wavelets based rotation invariant features," *Pattern Recognit. Lett.*, vol. 27, no. 16, pp. 1976–1982, Dec. 2006.

[5] D. R. Nayak, R. Dash, and B. Majhi, "Brain MR image classification using two-dimensional discrete wavelet transform and AdaBoost with random forests," *Neurocomputing*, vol. 177, pp. 188–197, Feb. 2016.

[6] G. Latif, M. M. Butt, A. H. Khan, O. Butt, and D. N. F. A. Iskandar, "Multiclass brain glioma tumor classification using block-based 3D wavelet features of MR images," in *Proc. 4th Int. Conf. Elect. Electron. Eng. (ICEEE)*, Apr. 2017, pp. 333–337.

[7] C. Wang, L. Lan, Y. Zhang, and M. Gu, "Face recognition based on principle component analysis and support vector machine," in *Proc. 3rd Int. Workshop Intell. Syst. Appl. (ISA)*, 2011, pp. 1–4.

[8] G. L. Qurat-Ul-Ain, S. B. Kazmi, M. A. Jaffar, and A. M. Mirza, "Classification and segmentation of brain tumor using texture analysis," in *Proc. Recent Adv. Artif. Intell., Knowl. Eng. Data Bases*, 2010, pp. 147–155.

[9] Y.-D. Zhang, S. Chen, S.-H. Wang, J.-F. Yang, and P. Phillips, "Magnetic resonance brain image classification based on weighted-type fractional Fourier transform and nonparallel support vector machine," *Int. J. Imag. Syst. Technol.*, vol. 25, no. 4, pp. 317–327, 2015.

[10] H. Mohsen, El-S. A. El-Dahshan, El-S. M. El-Horbaty, and A.-B. M. Salem, "Classification using deep learning neural networks for brain tumors," *Future Comput. Inform. J.*, vol. 3, no. 1, pp. 68–71, 2018.

[11] N. B. Bahadure, A. K. Ray, and H. P. Thethi, "Image analysis for MRI based brain tumor detection and feature extraction using biologically inspired BWT and SVM," *Int. J. Biomed. Imag.*, vol. 2017, Mar. 2017, Art. no. 9749108.

[12] J. Amin, M. Sharif, M. Yasmin, and S. L. Fernandes, "A distinctive approach in brain tumor detection and classification using MRI," *Pattern Recognit. Lett.*, 2017.

[13] A. Shenbagarajan, V. Ramalingam, C. Balasubramanian, and S. Palanivel, "Tumor diagnosis in MRI brain image using ACM segmentation and ANN-LM classification techniques," *Indian J. Sci. Technol.*, vol. 9, no. 1, pp. 1–12, 2016.

[14] X. Zhou *et al.*, "Detection of pathological brain in MRI scanning based on wavelet-entropy and naive Bayes classifier," in *Proc. Int. Conf. Bioinf. Biomed. Eng.*, Cham, Switzerland: Springer, Apr. 2015, pp. 201–209.

[15] R. Gurusamy and V. Subramaniam, "A machine learning approach for MRI brain tumor classification," *Comput., Mater. Continua*, vol. 53, no. 2, pp. 91–108, 2017.

[16] H. J. Aerts *et al.*, "Decoding tumour phenotype by noninvasive imaging using a quantitative radiomics approach," *Nature Commun.*, vol. 5, Jun. 2014, Art. no. 4006.

[17] Y. Li *et al.*, "MRI features can predict EGFR expression in lower grade gliomas: A voxel-based radiomic analysis," *Eur. Radiol.*, vol. 28, no. 1, pp. 356–362, 2018.

[18] J. J. Corso, E. Sharon, S. Dube, S. El-Saden, U. Sinha, and A. Yuille, "Efficient multilevel brain tumor segmentation with integrated Bayesian model classification," *IEEE Trans. Med. Imag.*, vol. 27, no. 5, pp. 629–640, May 2008.

[19] S. Pereira, J. Festa, J. A. Mariz, N. Sousa, and C. A. Silva, "Automatic brain tissue segmentation of multi-sequence MR images using random decision forests," in *Proc. MICCAI Grand Challenge MR Brain Image Segmentation*, 2013, pp. 1–7.

[20] T. Kalaiselvi and P. Nagaraja, "An automatic segmentation of brain tumor from MRI scans through wavelet transformations," *Int. J. Image, Graph. Signal Process.*, vol. 8, no. 11, pp. 59–65, 2016.

[21] M. A. Jaffar, Q. Ain, and T. S. Choi, "Tumor detection from enhanced magnetic resonance imaging using fuzzy curvelet," *Microsc. Res. Techn.*, vol. 75, no. 4, pp. 499–504, 2012.
[22] G. Shobana and R. Balakrishnan, "Brain tumor diagnosis from MRI feature analysis—A comparative study," in *Proc. Int. Conf. Innov. Inf., Embedded Commun. Syst. (ICIIECS)*, Mar. 2015, pp. 1–4.
[23] G. B. Praveen and A. Agrawal, "Multi stage classification and segmentation of brain tumor," in *Proc. 3rd Int. Conf. Comput. Sustain. Global Develop.*, Mar. 2016, pp. 1628–1632.
[24] M. Helén and T. Virtanen, "Audio query by example using similarity measures between probability density functions of features," *EURASIP J. Audio, Speech, Music Process.*, vol. 2010, pp. 1–12, Dec. 2010.
[25] G. N. Srinivasan and G. Shobha, "Statistical texture analysis," in *Proc. World Acad. Sci., Eng. Technol.*, vol. 36, pp. 1264–1269, Dec. 2008.
[26] J.-J. Aucouturier, M. Aurnhammer, and F. Pachet, "Second-order statistics are less important for audio textures than for image textures," *IEEE Trans. Speech Audio Process.*, pp. 14–25, 2008.
[27] P. Singh, P. Singh, and R. K. Sharma, "JPEG image compression based on biorthogonal, coiflets and daubechies wavelet families," *Int. J. Comput. Appl.*, vol. 13, no. 1, pp. 1–7, 2011.
[28] G. Latif, D. N. F. A. Iskandar, J. Alghazo, and A. Jaffar, "Improving brain MR image classification for tumor segmentation using phase congruency," *Current Med. Imag. Rev.*, vol. 14, no. 6, pp. 914–922, 2018.
[29] B. H. Menze *et al.*, "The multimodal brain tumor image segmentation benchmark (BRATS)," *IEEE Trans. Med. Imag.*, vol. 34, no. 10, pp. 1993–2024, Oct. 2015.
[30] D. Summers, "Harvard whole brain atlas: www.med.harvard.edu/AANLIB/home.html," *J. Neurol., Neurosurg. Psychiatry*, vol. 74, no. 3, p. 288, 2003.
[31] M. Nazir, F. Wahid, and S. A. Khan, "A simple and intelligent approach for brain MRI classification," *J. Intell. Fuzzy Syst.*, vol. 28, no. 3, pp. 1127–1135, 2015.
[32] M. Havaei, P.-M. Jodoin, and H. Larochelle, "Efficient interactive brain tumor segmentation as within-brain kNN classification," in *Proc. 22nd Int. Conf. Pattern Recognit. (ICPR)*, Aug. 2014, pp. 556–561.

GHAZANFAR LATIF received the B.S. degree (Hons.) in computer science from the FAST National University of Computer and Emerging Sciences, Pakistan, in 2010, and the M.S. degree in computer science from the King Fahd University of Petroleum and Minerals, Saudi Arabia, in 2014. He was an Instructor with Prince Mohammad Bin Fahd University, Saudi Arabia, where he was with the Computer Science Department for three years and has two years industry work experience. He is currently a Ph.D. Scholar with the University of Malaysia Sarawak, Malaysia. Throughout his educational carrier, he has a number of achievements like full scholarships for FSc, BS-CS, and MS-CS. His research interests include image processing, artificial intelligence, neural networks, and medical image processing.

D. N. F. AWANG ISKANDAR received the bachelor's degree (Hons.) in information technology majoring in computational science, the master's degree in multimedia computing, and the Ph.D. degree in computer science from the Biomedical Informatics Systems Engineering Laboratory. She was involved in the EU funded project—Combining and Uniting Business Intelligence with Semantic Technologies. She is currently a Senior Lecturer with the Faculty of Computer Science and Information Technology, UNIMAS Sarawak. She is focused on techniques for querying an image collection including: fusing text accompanying the images with visual features, automatic region tagging, and using ontology to enrich the semantic meaning of tagged image regions leading to the bridging of semantic gap in content-based image retrieval. Her current research focuses on minimizing the gap between image features and high-level semantics in medical and agricultural content-based image retrieval systems. She is currently the Principle Investigator for several grants provided by the Ministry of Education and had successfully completed one Science Fund Grant from the Ministry of Science, Technology and Innovation.

JAAFAR M. ALGHAZO received the M.Sc. and Ph.D. degrees in computer engineering from Southern Illinois University Carbondale, in 2000 and 2004, respectively. He joined Prince Mohammad Bin Fahd University (PMU) as the Founding Dean of the College of Computer Engineering and Science and held various positions including the Dean of Graduate Studies and Research, the Dean of Institutional Relations, and the Dean of Continuing Education and Community Service. He is currently an Assistant Professor with PMU. His research interests include the modeling and realization of biological mechanism using CAD and field-programmable gate arrays (FPGAs), the modeling and realization of arithmetic operations using CAD and FPGAs, low-power cache design, and assistive technology for students with disabilities.

NAZEERUDDIN MOHAMMAD received the B.E. degree in electronics and communications engineering from Osmania University, India, in 1996, the M.S. degree in systems engineering from the King Fahd University of Petroleum and Minerals (KFUPM), Saudi Arabia, in 1999, the Honours Diploma degree in software development from BDPS, India, in 1997, and the Ph.D. degree from the School of Computing and Information Engineering, University of Ulster, Coleraine, U.K., in 2007. He also received practical training at BDPS, in 1997. He was an IT Infrastructure Manager/Administrator and a Lecturer with KFUPM, a Postgraduate Researcher with the University of Ulster, a Research Intern with Cisco Systems, USA, and an IT Infrastructure Manager/Administrator and a Researcher with the Portland House Research Group, Australia. He received the M.S. Research Scholarship from KFUPM, in 1997, the Vice Chancellors Research Scholarship from the University of Ulster, in 2004, and the First Prize from the Faculty of Engineering Business Plan Competition at the University of Ulster, in 2006.